

## Research Article

# Effect of Solvents and Stabilizer Molar Ratio on the Growth Orientation of Sol-Gel-Derived ZnO Thin Films

R. Bekkari<sup>1</sup>, B. Jaber,<sup>2</sup> H. Labrim<sup>1</sup>, M. Ouafi<sup>1</sup>, N. Zayyoun,<sup>1</sup> and L. Laânab<sup>1</sup>

<sup>1</sup>LCS, Faculty of Science, Mohammed V University, Rabat, Morocco

<sup>2</sup>Materials Science Platform, UATRS Division, CNRST, Rabat, Morocco

<sup>3</sup>CNESTEN, B.P. 1382 R.P. 10001, Rabat, Morocco

Correspondence should be addressed to R. Bekkari; [bekkarirabab@gmail.com](mailto:bekkarirabab@gmail.com)

Received 10 September 2018; Accepted 1 January 2019; Published 21 February 2019

Academic Editor: Mahmoud M. El-Nahass

Copyright © 2019 R. Bekkari et al. This is an open access article distributed under the Creative Commons Attribution License, which permits unrestricted use, distribution, and reproduction in any medium, provided the original work is properly cited.

This work targets to control the growth orientation of sol-gel-derived ZnO thin films in order to allow different modes of excitation (longitudinal and transverse) when targeted to be used in piezoelectric applications. For that, the effect of solvents and stabilizer molar ratio on the structural and optical characteristics of the obtained films is investigated by means of X-ray diffraction (XRD), scanning electron microscopy (SEM), and UV-Vis spectrophotometry. The XRD results show clearly that the synthesized films exhibit hexagonal wurtzite structure without any secondary phases and that the crystallite average size, estimated by the Scherrer formula, is ranged between 13 and 30 nm. The main finding of this work is to show that the control of the crystalline growth orientation is possible simply by varying the solvent nature and/or the stabilizer molar ratio. These later parameters are therefore considered as key factors when seeking to develop the ZnO-based transducers. Actually, the ZnO thin films synthesized with propanol as solvent are oriented only along the *c*-axis; meanwhile, when using the isopropanol or ethanol, other preferential orientations appear. Additionally, the effect of MEA molar ratio (*r*) has been studied on the propanol-derived films (the unfavorable case). It has been found that this parameter has a direct effect on the crystalline growth orientation of these films and that a new preferential orientation (100) appears at low *r*. On the other hand, SEM images show the formation of homogeneous nanocrystalline thin films with an average grain size ranged between 19 and 35 nm. Moreover, the ZnO thin films exhibit a high transparency in the visible region, and the measured transmittance is ranged from 85 to 97%. However, the change of ZnO film orientation has no significant effect on the direct bandgap energy which is closed to 3.30 eV.

## 1. Introduction

Zinc oxide (ZnO) is one of the more attractive semiconducting metal oxides owing to its interesting properties including a wide and direct bandgap (3.37 eV) and large exciton binding energy (60 meV) as well as high transparency [1–6]. For that, ZnO thin film is an excellent candidate for many applications, such as transparent electrodes [7], ultra-violet photoconductive detectors [8], piezoelectric transducers [9], gas sensors [10], and solar cell [11–13]. The hardware requirements of these applications are behind the development of various ZnO growing techniques including chemical bath deposition [14], sputtering [15], electron beam evaporation [16], spray pyrolysis [17, 18], and the sol-gel

method [19, 20]. Among all these, the sol-gel is a low-cost method which has several advantages such as the high surface morphology at low crystallization temperature, the easy control of chemical components, and the fabrication of large area.

ZnO films can be produced in wurtzite (hcp), rock salt (fcc), and zincblende (fcc) phases [21]. In the ambient conditions, ZnO crystallizes in the wurtzite phase which is a tetrahedrally coordinated structure with hexagonal lattice. In this phase, due to its noncentrosymmetric characteristics, ZnO films exhibit piezoelectric properties, which can be exploited in transducer applications [22]. For that, the piezoelectric layer must be correctly oriented with respect to the electrodes so that the acoustic wave can be

excited [23, 24]. Two types of acoustic waves are distinguished according to the atom displacement in relation to the direction of the wave propagation: longitudinal waves, whose particle displacement is parallel to the direction of wave propagation, and transverse waves, for which the particle displacement is perpendicular to the direction of wave propagation [25]. As it is known, ZnO thin films grow preferentially along their crystallographic *c*-axis, allowing only longitudinal mode excitation [26]. One of the major challenges, when seeking to improve the ZnO piezoelectric properties for transducer applications, is to also allow the excitation of transverse mode. The control of the growth orientations is important because it allows predicting which types of acoustic waves can be generated within the thin layer of the material. Therefore, making ZnO to grow along other orientations is a key factor to develop ZnO-based transducers which can be excited both in longitudinal and transverse modes.

The quality of the ZnO films is typically determined regarding surface uniformity, transparency, conductivity, and crystalline orientation [27]. This quality is strongly affected by many factors such as the sol aging time [28, 29], the concentration of the precursor [30–33], and the preheating and the postannealing temperatures [31, 34, 35]. In our previous paper [19], we studied the influence of the precursor concentration and annealing treatment on the structural and optical properties of sol-gel ZnO thin films. The results confirmed clearly that the synthesis parameters affect both the film orientation and the crystal quality. In this framework, the objective of this work is to control the growth orientation of sol-gel-derived ZnO thin films in order to allow different modes of excitation (longitudinal and transverse) when used in piezoelectric applications. To this end, the effect of solvent nature (propanol, isopropanol, and ethanol) and the stabilizer molar ratios on the structural and optical properties of ZnO thin films is investigated and discussed.

## 2. Experimental Details

ZnO thin films are prepared by the sol-gel process. As a starting material, the precursor sol (0.1 M) is prepared by dissolving zinc acetate dihydrate  $[Zn(CH_3COO)_2 \cdot 2H_2O]$  in different solvents, namely, propanol, isopropanol, and ethanol. The solution was heated at 60°C for one hour and then the MEA stabilizer is added drop by drop. The MEA to zinc acetate molar ratio (*r*) is varied from 0.5 to 2. A clear homogeneous solution is obtained after one hour of reaction. The ZnO films were deposited on the glass substrates by spin coating at 3000 rpm for 30 s under normal conditions of temperature and pressure. To remove organic matter, the as-synthesized films were preheated in air at 200°C for 10 min. The coating and the preheating treatment processes are repeated several times to achieve the desired thickness. Finally, the films are subsequently annealed at 500°C to improve the crystallization and the densification.

The grown ZnO thin films were investigated by a Panalytical X'Pert Pro X-ray Diffractometer, working in Bragg-Brentano geometry with Cu-K $\alpha$  radiation. The morphology study was performed using FEI Quanta 200 scanning

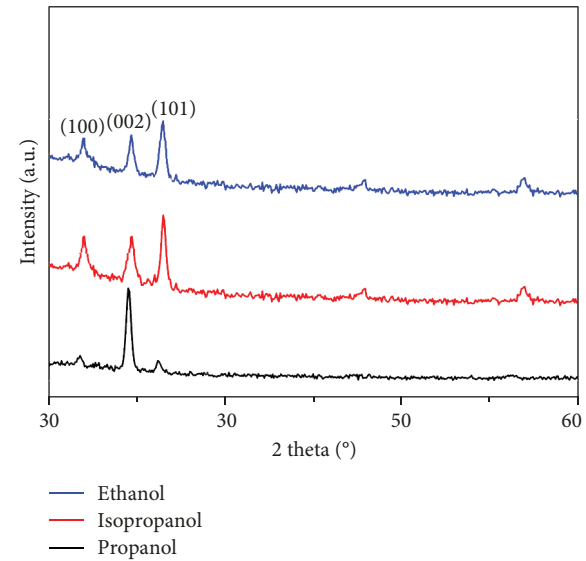


FIGURE 1: X-ray diffraction patterns of ZnO thin films synthesized with various solvents.

electron microscopy (SEM). The optical transmittances and bandgap energies of the samples were carried out using a PerkinElmer Lambda 900 Spectrophotometer in the UV-Vis-NIR regions.

## 3. Results and Discussion

### 3.1. Effect of Solvent

**3.1.1. Structural Study.** Figure 1 shows XRD patterns of ZnO thin films obtained using different solvents (ethanol, isopropanol, and propanol) when the Zn concentration was fixed to 0.5 M. All recorded peaks show that the samples exhibit hexagonal wurtzite structure (JCPDS 36-1451) without any other secondary phases. It is obvious that the ZnO thin films synthesized with isopropanol and ethanol exhibit the highest (101) peak intensities. However, when the propanol is used as solvent, the highest intensities are obtained for the (002) peak. These results show that it is possible to control the preferential growth axis of ZnO thin films by varying solvent and that the isopropanol is the best one.

To qualify the preferred orientation of the obtained ZnO films, the relative intensity  $I_{r(hkl)}$  is evaluated using the following relationship:

$$I_{r(hkl)} = \frac{I_{hkl}}{\sum I_{hkl}}, \quad (1)$$

where  $I_{hkl}$  is the (hkl) peak intensity and  $\sum I_{hkl}$  is the sum of the intensities of all the diffraction peaks.

Figure 2 presents the variation of the relative intensity ratio as a function of solvent nature. It is obvious that the film synthetized using propanol as solvent is preferentially oriented along (002) direction, while those prepared using isopropanol or ethanol behave as the bulk. This behavior perhaps linked to the boiling point of the chosen solvent

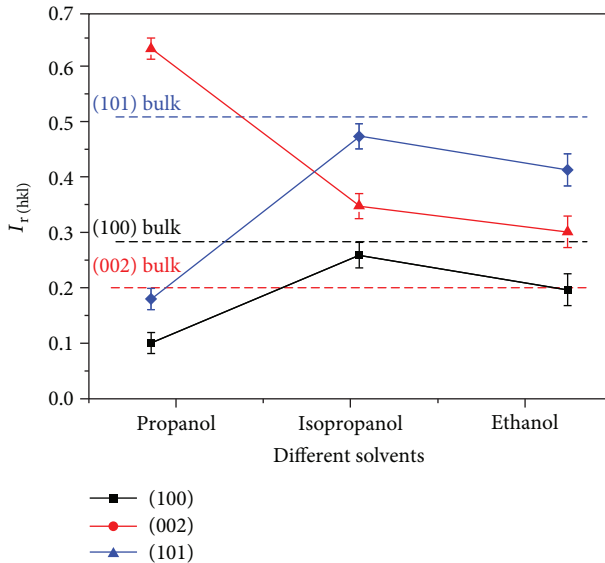


FIGURE 2: Relative intensity ratio of ZnO films obtained using different solvents.

(propanol 98°C, isopropanol 82.6°C, and ethanol 78.37°C) [36]. In fact, the solvent with a higher boiling point evaporates more slowly during heating (60°C) and would promote the growth along the natural preferential *c*-axis orientation. Meanwhile, in the case of lower boiling point solvents, the evaporation is faster and forces the material to grow along other orientations and behaves as the bulk.

The crystallite size (*D*) of the ZnO thin films is estimated by the Debye-Scherrer formula as follows:

$$D = \frac{0.9\lambda}{\beta \cos \theta}, \quad (2)$$

where  $\lambda$  is the wavelength of the used X-ray radiation;  $\beta$  is the full width at half maximum (FWHM), and  $2\theta$  is the highest diffraction angle. We could have more crystal quality information using the following formula:

$$\delta = \frac{1}{D^2}, \quad (3)$$

where  $\delta$  is the dislocation density.

The microstrain in the films was calculated from the formula given as follows:

$$\varepsilon = \frac{\beta \cos \theta}{4}. \quad (4)$$

The lattice constants *a* and *c* of the ZnO wurtzite structure are calculated using Bragg's law as follows:

$$a = \frac{\lambda}{\sqrt{3} \cdot \sin \theta}, \quad (5)$$

$$c = \frac{\lambda}{\sin \theta}.$$

All the obtained values are given in Table 1. It was observed that the ZnO thin films prepared using propanol present the smallest crystallite size (16 nm) while those prepared using isopropanol present the largest ones (30 nm) and then the smallest dislocation density (better crystallization). In addition, the evaluated strain decreases as the crystallite size increases; this is may be due to the decrease of grain boundary area [37]. The largest crystallite size obtained in the case of isopropanol is attributed to its highest viscosity when compared to the two other solvents [36]. The lattice parameters “*a*” and “*c*” values are closest to the pure bulk ZnO (JCPDS card 36-1451). This indicates that the obtained ZnO films are of good crystallinity.

A typical SEM image of the isopropanol-derived ZnO thin films is presented in Figure 3; it shows that the surface of the film is smooth and dense, which means a good crystalline quality of the film. The grain size is uniformly distributed with an average of about 35 nm.

**3.1.2. Optical Study.** The optical transmittance spectra of the obtained ZnO thin films using propanol, isopropanol, and ethanol as solvents are presented in Figure 4. As shown, all the films exhibit an average transmission higher than 90% in the visible region. These optical measurements indicate that the films have good crystalline quality which has also been confirmed by XRD analysis. The observed interference fringes are due to multiple reflections of radiation on two film interfaces, i.e., at the film/air and the film/substrate interfaces. This behavior shows that the films studied have smooth and uniform surfaces as observed by SEM.

The optical absorption coefficient ( $\alpha$ ) can be calculated using the Lambert law relation as follows:

$$\alpha = \frac{1}{d} \ln \left( \frac{1}{T} \right), \quad (6)$$

where  $d$  is the thickness of the film and  $T$  is the transmittance.

The relation between absorption coefficient and incident photon energy can be written as follows:

$$\alpha h\nu = A (h\nu - E_g)^{1/2}, \quad (7)$$

where  $h\nu$  is the photon energy,  $A$  is constant for direct transition, and  $E_g$  is the direct bandgap. The obtained values of the bandgap energy and thickness of the films for different solvents are presented in Table 2. Lowest bandgap energy (3.25 eV) is observed in the case of propanol. As confirmed by XRD results, this effect is seemingly attributed to the strain generation which leads to the variation in the interatomic spacing [38].

We conclude that the isopropanol and ethanol are the appropriate solvents for controlling the growth orientation of ZnO thin films and that the isopropanol is the most preferred for producing the ZnO films with suitable structural and optical properties.

**3.2. Effect of Stabilizer Molar Ratio.** As it can be deduced from the last paragraph, the propanol-derived films were

TABLE 1: Evaluated structural parameters of ZnO thin films compared with the bulk ones.

Solvent	$D$ (nm)	$\mathcal{E} \times 10^{-3}$ (%)	$\delta \times 10^{-3}(\text{nm})^{-2}$	$a$ ( $\text{\AA}$ )	$c$ ( $\text{\AA}$ )
Propanol	$16 \pm 8$	2.01	3.91	$3.251 \pm 0.001$	$5.201 \pm 0.006$
Isopropanol	$30 \pm 10$	1.41	1.11	$3.255 \pm 0.003$	$5.212 \pm 0.001$
Ethanol	$22 \pm 6$	1.95	2.07	$3.242 \pm 0.001$	$5.216 \pm 0.004$
ZnO bulk	—	—	—	3.249	5.206

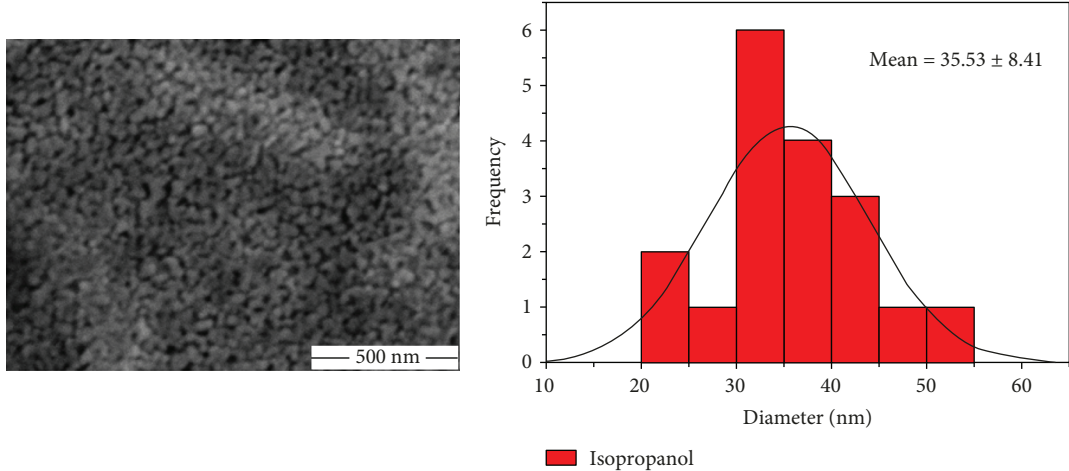


FIGURE 3: SEM image and particle size distribution of the ZnO thin films obtained using isopropanol as solvent.

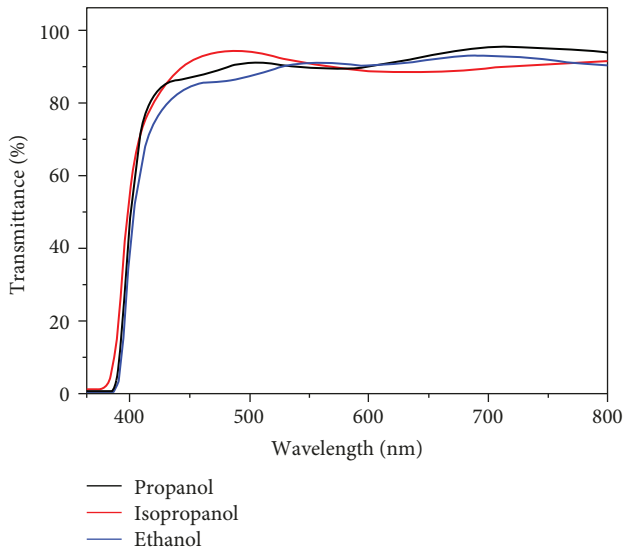


FIGURE 4: UV-Vis transmittance spectra of the ZnO thin films with various solvents used.

TABLE 2: The calculated values of the optical bandgap and thicknesses of the films for different solvents.

Solvent	$d$ (nm)	$E_g$ (eV)
Propanol	367	3.25
Isopropanol	353	3.30
Ethanol	377	3.27

oriented only along the  $c$ -axis which constitutes the unfavorable case. In order to make them growing along other orientations, the effect of different molar ratio ( $r$ ) MEA to Zn is investigated.

**3.2.1. Structural Study.** The XRD patterns of the propanol-derived ZnO films with different MEA molar ratios are shown in Figure 5. All the diffraction peaks are indexed and match with the pure hexagonal wurtzite structure without any secondary phases. As can be observed, when increasing the MEA molar ratio from 1 to 2, only high intense (002) peak is observed, indicating that the film crystallinity has been improved along  $c$ -axis orientation. Meanwhile, when decreasing the MEA molar ratio from 1 to 0.5, the (100) peak intensity increases to the detriment of (002) peak, indicating the apparition of another preferential orientation.

To more illustrate the effect of the stabilizer molar ratio on the crystalline growth orientation, we present in Figure 6 the variation of the relative intensities  $I_{r(hkl)}$  versus the stabilizer molar ratio. It is clear that the relative intensity ratio of (100) increases and that of (002) decreases with decreasing MEA molar ratio. This result indicates that it is possible to change the preferential orientation by varying MEA molar ratio and then both (100) and (002) are considered as preferential orientations at low  $r$ . Additionally, it has been reported [39] that the function of complexing agent (MEA) is to promote the  $\text{Zn}^{2+}$  condensation and favors the formation of ZnO owing to the presence of amine which

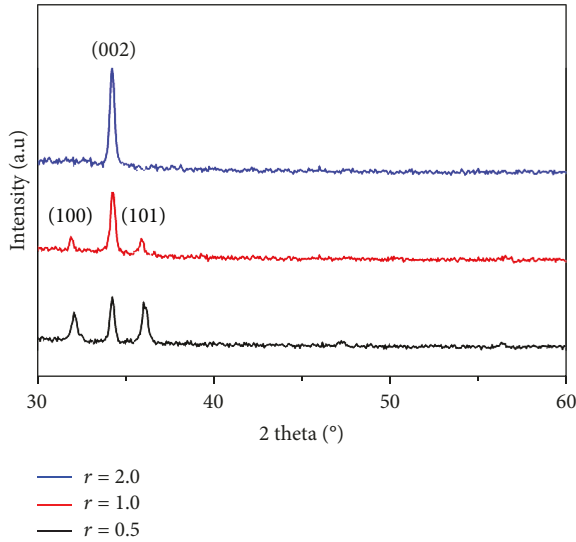


FIGURE 5: XRD patterns of ZnO thin films prepared at different stabilizer molar ratios.

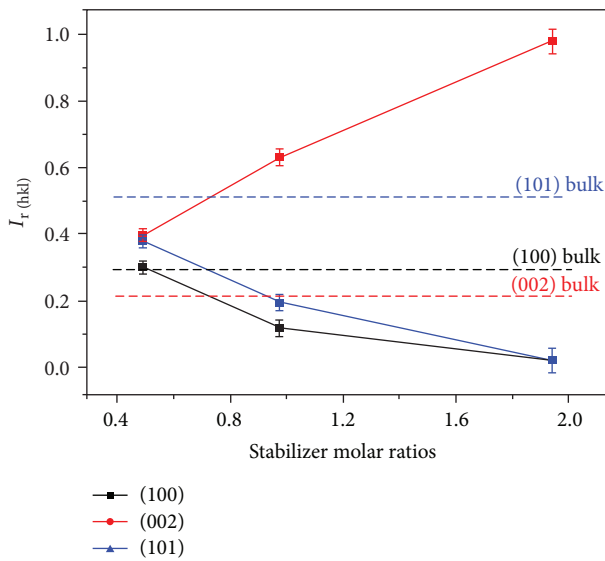


FIGURE 6: Relative intensity ratio of ZnO films obtained using different stabilizer molar ratios.

increases the pH of the solution. Thereby, the lower ratios of MEA would decrease the  $Zn^{2+}$  condensation rate in the (002) plane (of low surface free energy) and finally improve the growth along other orientations as (100). Comparable results were obtained by Bekkari et al. [3].

The structural parameters of samples calculated by different formulas are presented in Table 3. A good agreement with the ZnO bulk, in terms of lattice parameters, is observed. However, the crystallite size remains constant regardless the MEA molar ratios.

Figure 7 presents a typical SEM image of ZnO thin films obtained at  $r = 0.5$ . Relatively smooth surface with homogeneous and uniform grains is observed on the image. The grain average size is about 19 nm.

TABLE 3: Evaluated structural parameters of the propanol-derived ZnO films at different MEA molar ratios compared with the bulk.

Stabilizer molar ratio ( $r$ )	$D$ (nm)	$a$ (Å)	$c$ (Å)
0.5	$19 \pm 5$	$3.255 \pm 0.003$	$5.210 \pm 0.001$
1.0	$16 \pm 8$	$3.251 \pm 0.001$	$5.201 \pm 0.006$
2.0	$13 \pm 6$	—	$5.215 \pm 0.002$
ZnO bulk	—	3.249	5.206

**3.2.2. Optical Study.** Figure 8 shows the transmittance spectra of the propanol-derived ZnO films with different MEA molar ratios. A transmittance greater than 80% is obtained in the visible region for all ZnO thin films. Nevertheless, the transmission goes down from 97 to 85% when the molar ratio ( $r$ ) is varied from 0.5 to 2.0. This reduction of transmittance at higher MEA molar ratio may be attributed to the increase in thickness and/or to the reduction of ZnO layer density which are the results of an excessive evaporation of the MEA during the postdepot annealing treatment.

The values of the bandgap energy and thicknesses of the ZnO thin films are summarized in Table 4 for different MEA molar ratios. It is observed that the bandgap energy remains almost identical whatever the MEA molar ratio and very close to that of bulk ZnO (3.37 eV). On the other hand, the increase in MEA ratio induces an augmentation in the solution viscosity which raises the deposition rate and consequently increases the thickness of the film.

We conclude that the MEA molar ratio has a direct effect on the crystalline growth orientation and optical properties.  $r = 0.5$  is the optimized MEA value which allows different growth orientations associated to the best optical properties.

#### 4. Conclusion

In summary, the effects of the solvents and stabilizer molar ratio on the structural and optical properties of sol-gel-derived ZnO thin films have been studied and discussed. X-ray diffraction results confirm clearly that the synthesized films exhibit hexagonal wurtzite structure without any secondary phases, and then it is possible to control the preferential growth axis of ZnO thin films by varying solvents as well as the MEA molar ratio. The films synthesized by using propanol as solvent are preferentially oriented along the (002) direction, while in those prepared by using isopropanol or ethanol, other preferential orientations are observed. The effect of MEA molar ratio is studied on the propanol-derived films which are oriented only along the  $c$ -axis (the unfavorable case). It was found that the MEA molar ratio has a direct effect on the crystalline growth orientation of these films and that a new preferential orientation (100) appears at low  $r$ . These results are of great importance when these films are designed for piezoelectric transducer applications. Likewise, the SEM results confirm that the obtained films are homogeneous, continuous with spherical nanosized crystallites. Additionally, UV visible transmittance

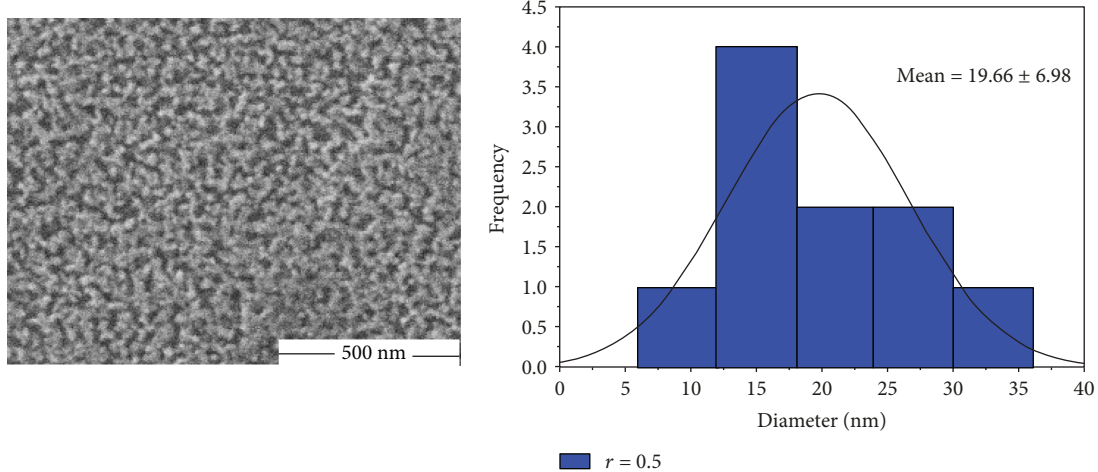


FIGURE 7: SEM image and particle size distribution of the ZnO thin films obtained using  $r = 0.5$ .

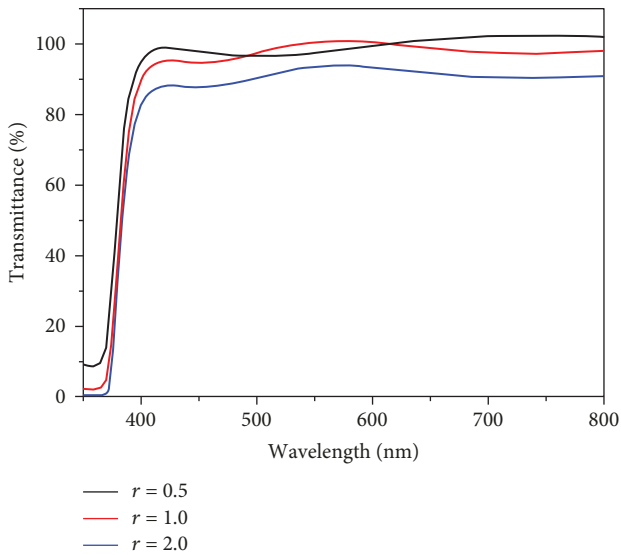


FIGURE 8: Optical transmittance spectra of ZnO thin films deposited at different stabilizer molar ratios.

TABLE 4: Values of the optical gap and thickness as a function of the stabilizer molar ratio for ZnO thin films obtained when propanol is used as solvent.

Stabilizer molar ratio ( $r$ )	$d$ (nm)	$E_g$ (eV)
0.5	278	3.28
1.0	347	3.27
2.0	386	3.27

spectra indicate that the films are highly transparent (>80%) in the visible region. The measured bandgap values of the obtained ZnO films are between 3.25 and 3.30 eV that is in good agreement with literature values.

## Data Availability

The data used to support the findings of this study are included within the article.

## Conflicts of Interest

The authors declare that they have no conflicts of interest.

## References

- [1] D. Djouadi, A. Chelouche, and A. Aksas, "Amplification of the UV emission of ZnO: Al thin films prepared by sol-gel method," *Journal of Materials and Environmental Science*, vol. 3, pp. 585–590, 2012.
- [2] M. M. Ali and S. M. Meshari, "Structural and optical characterization of ZnO thin films by sol-gel technique," *Journal of Basrah Researches*, vol. 40, no. 1A, pp. 39–48, 2014.
- [3] R. Bekkari, L. Laâab, D. Boyer, R. Mahiou, and B. Jaber, "Influence of the sol gel synthesis parameters on the photoluminescence properties of ZnO nanoparticles," *Materials Science in Semiconductor Processing*, vol. 71, pp. 181–187, 2017.
- [4] N. Shakti and P. S. Gupta, "Structural and optical properties of sol-gel prepared ZnO thin film," *Applied Physics Research*, vol. 2, no. 1, p. 19, 2010.
- [5] A. Farooq and M. Kamran, "Effect of sol concentration on structural and optical behavior of ZnO thin films prepared by sol-gel spin coating," *International Journal of Applied Physics and Mathematics*, vol. 2, pp. 430–432, 2012.
- [6] H. F. Hussein, G. M. Shabeb, and S. S. Hashim, "Preparation ZnO thin film by using sol-gel-processed and determination of thickness and study optical properties," *Journal of Materials and Environmental Science*, vol. 2, no. 4, pp. 423–426, 2011.
- [7] J. Zhou, X. Z. Wu, D. B. Xiao et al., "Deposition of aluminum doped ZnO as electrode for transparent ZnO/glass surface acoustic wave devices," *Surface & Coatings Technology*, vol. 320, pp. 39–46, 2017.
- [8] Z. Ke, Z. Yang, M. Wang, M. Cao, Z. Sun, and J. Shao, "Low temperature annealed ZnO film UV photodetector with fast photoresponse," *Sensors and Actuators A: Physical*, vol. 253, pp. 173–180, 2017.
- [9] K. Maeda, M. Sato, I. Niikura, and T. Fukuda, "Growth of 2 inch ZnO bulk single crystal by the hydrothermal method," *Semiconductor Science and Technology*, vol. 20, no. 4, pp. S49–S54, 2005.

- [10] V. L. Patil, S. A. Vanalakar, P. S. Patil, and J. H. Kim, "Fabrication of nanostructured ZnO thin films based NO<sub>2</sub> gas sensor via SILAR technique," *Sensors and Actuators B: Chemical*, vol. 239, pp. 1185–1193, 2017.
- [11] M. Hála, H. Kato, M. Algasinger et al., "Improved environmental stability of highly conductive nominally undoped ZnO layers suitable for n-type windows in thin film solar cells," *Solar Energy Materials & Solar Cells*, vol. 161, pp. 232–239, 2017.
- [12] B. J. Jin, S. Im, and S. Y. Lee, "Violet and UV luminescence emitted from ZnO thin films grown on sapphire by pulsed laser deposition," *Thin Solid Films*, vol. 366, no. 1-2, pp. 107–110, 2000.
- [13] Y. Qu, X. Huang, Y. Li et al., "Chemical bath deposition produced ZnO nanorod arrays as an antireflective layer in the polycrystalline Si solar cells," *Journal of Alloys and Compounds*, vol. 698, pp. 719–724, 2017.
- [14] Z. Ye, T. Wang, S. Wu, X. Ji, and Q. Zhang, "Na-doped ZnO nanorods fabricated by chemical vapor deposition and their optoelectrical properties," *Journal of Alloys and Compounds*, vol. 690, pp. 189–194, 2017.
- [15] Y. Zhang, G. du, D. Liu et al., "Crystal growth of undoped ZnO films on Si substrates under different sputtering conditions," *Journal of Crystal Growth*, vol. 243, no. 3-4, pp. 439–443, 2002.
- [16] J. Sun, M. A. Yarmolenko, A. A. Rogachev et al., "Investigation of structural properties of electron-beam deposition of zinc oxide coatings doped with copper," *Surfaces and Interfaces*, vol. 6, pp. 24–32, 2017.
- [17] S. A. Salman, S. Q. Hazza, and S. J. Abbas, "Effect of Sn Doping on Structural and Electrical Properties of ZnO Thin Films Prepared by Chemical Spray Pyrolysis Method," *Invention Journal of Research Technology in Engineering & Management (IJRTEM)*, vol. 41, pp. 1–5, 2017.
- [18] M. Imai, M. Watanabe, A. Mochihara et al., "Atmospheric growth of ZnO films deposited by spray pyrolysis using diethylzinc solution," *Journal of Crystal Growth*, vol. 468, pp. 473–476, 2017.
- [19] B. Jaber, L. Laanab, and R. Bekkari, "Influence of precursor concentration and annealing treatment on the structural and optical properties of sol gel ZnO thin films," *Moroccan Journal of Chemistry*, vol. 4, no. 2, pp. 289–298, 2016.
- [20] F. J. Serrao, K. M. Sandeep, and S. M. Dharmaprakash, "Annealing-induced modifications in sol-gel spin-coated Ga:ZnO thin films," *Journal of Sol-Gel Science and Technology*, vol. 78, no. 2, pp. 438–445, 2016.
- [21] A. M. P. Santos and E. J. P. Santos, "Pre-heating temperature dependence of the c-axis orientation of ZnO thin films," *Thin Solid Films*, vol. 516, no. 18, pp. 6210–6214, 2008.
- [22] T. Shiosaki and A. Kawabata, "Low-frequency piezoelectric-transducer applications of ZnO film," *Applied Physics Letters*, vol. 25, no. 1, pp. 10–11, 1974.
- [23] A. Khan, Z. Abas, H. Soo Kim, and I.-K. Oh, "Piezoelectric thin films: an integrated review of transducers and energy harvesting," *Smart Materials and Structures*, vol. 25, no. 5, article 053002, 2016.
- [24] B. A. Buchine, W. L. Hughes, F. L. Degertekin, and Z. L. Wang, "Bulk acoustic resonator based on piezoelectric ZnO belts," *Nano Letters*, vol. 6, no. 6, pp. 1155–1159, 2006.
- [25] K. Uchino, "International Center for Actuators and Transducers," in *Penn State University, Report, International Center for Actuators and Transducers, Penn State University*, p. 40, University Park, PA, USA, 2003.
- [26] H. F. Pang, Y. Q. Fu, R. Hou et al., "Annealing effect on the generation of dual mode acoustic waves in inclined ZnO films," *Ultrasonics*, vol. 53, no. 7, pp. 1264–1269, 2013.
- [27] M. F. Malek, M. H. Mamat, Z. Khusaimi et al., "Sonicated sol-gel preparation of nanoparticulate ZnO thin films with various deposition speeds: the highly preferred c-axis (0 0 2) orientation enhances the final properties," *Journal of Alloys and Compounds*, vol. 582, pp. 12–21, 2014.
- [28] S. M. Rozati, S. Moradi, S. Golshahi, R. Martins, and E. Fortunato, "Electrical, structural and optical properties of fluorine-doped zinc oxide thin films: effect of the solution aging time," *Thin Solid Films*, vol. 518, no. 4, pp. 1279–1282, 2009.
- [29] Y. Li, L. Xu, X. Li, X. Shen, and A. Wang, "Effect of aging time of ZnO sol on the structural and optical properties of ZnO thin films prepared by sol-gel method," *Applied Surface Science*, vol. 256, no. 14, pp. 4543–4547, 2010.
- [30] N. Saleem, "Effects of induced magnetic field and slip condition on peristaltic transport with heat and mass transfer in a non-uniform channel," *International Journal of the Physical Sciences*, vol. 7, no. 2, pp. 2971–2979, 2012.
- [31] S. Heinonen, J. P. Nikkanen, H. Hakola et al., "Effect of temperature and concentration of precursors on morphology and photocatalytic activity of zinc oxide thin films prepared by hydrothermal route," in *IOP Conference Series: Materials Science and Engineering*, vol. 123, pp. 1–6, Miskolc-Lillafüred, Hungary, 2016.
- [32] C. Amutha, A. Dhanalakshmi, B. Lawrence, K. Kulathuraan, V. Ramadas, and B. Natarajan, "Influence of Concentration on Structural and Optical Characteristics of Nanocrystalline ZnO Thin Films Synthesized by Sol-Gel Dip Coating Method," *Progress in Nanotechnology and Nanomaterials*, vol. 3, pp. 13–18, 2014.
- [33] N. Siregar, E. Marlianto, and S. Gea, "The effect of concentration of structure and optical properties of thin films synthesized by sol-gel methods spin coating," *International Journal of Sciences: Basic and Applied Research*, vol. 22, no. 1, pp. 428–434, 2015.
- [34] H. Belkhalfa, H. Ayed, A. Hafdallah, M. S. Aida, and R. T. Ighil, "Characterization and studying of ZnO thin films deposited by spray pyrolysis: effect of annealing temperature," *Optik*, vol. 127, no. 4, pp. 2336–2340, 2016.
- [35] D.-T. Phan and G.-S. Chung, "The effect of post-annealing on surface acoustic wave devices based on ZnO thin films prepared by magnetron sputtering," *Applied Surface Science*, vol. 257, no. 9, pp. 4339–4343, 2011.
- [36] K. L. Foo, M. Kashif, U. Hashim, and W. W. Liu, "Effect of different solvents on the structural and optical properties of zinc oxide thin films for optoelectronic applications," *Ceramics International*, vol. 40, no. 1, pp. 753–761, 2014.
- [37] A. Begum, A. Hussain, and A. Rahman, "Effect of deposition temperature on the structural and optical properties of chemically prepared nanocrystalline lead selenide thin films," *Beilstein Journal of Nanotechnology*, vol. 3, pp. 438–443, 2012.
- [38] F. Zahedi, R. S. Dariani, and S. M. Rozati, "Structural, optical and electrical properties of ZnO thin films prepared by spray pyrolysis: effect of precursor concentration," *Bulletin of Materials Science*, vol. 37, no. 3, pp. 433–439, 2014.
- [39] P. Sagar, P. K. Shishodia, and R. M. Mehra, "Influence of pH value on the quality of sol-gel derived ZnO films," *Applied Surface Science*, vol. 253, no. 12, pp. 5419–5424, 2007.

